THE JOURNAL OF PHYSICAL CHEMISTRY Letters

LETTER

pubs.acs.org/JPCL

Reactions of Ions with Ionic Liquid Vapors by Selected-Ion Flow Tube Mass Spectrometry

Steven D. Chambreau,[†] Jerry A. Boatz,[‡] Ghanshyam L. Vaghjiani,[*,‡] Jeffrey F. Friedman,[§,⊥,#] Nicole Eyet,[§,#,¶] and A. A. Viggiano[§]

[†]ERC, Inc. and [‡]Air Force Research Laboratory, AFRL/RZSP, Propulsion Directorate, Edwards Air Force Base, California, 93524, United States

[§]Air Force Research Laboratory, AFRL/RVBXT Space Vehicles Directorate, Hanscom Air Force Base, Massachusetts 01731, United States

[⊥]Department of Physics, University of Puerto Rico, Mayaguez, Puerto Rico 00681-9016

[#]Institute for Scientific Research, Boston College, Chestnut Hill, Massachusetts 02467, United States

[¶]Department of Chemistry, St. Anselm College, 100 Saint Anselm Drive, Manchester, New Hampshire 03102, United States

Supporting Information

ABSTRACT: Room-temperature ionic liquids exert vanishingly small vapor pressures under ambient conditions. Under reduced pressure, certain ionic liquids have demonstrated volatility, and they are thought to vaporize as intact cation−anion ion pairs. However, ion pair vapors are difficult to detect because their concentration is extremely low under these conditions. In this Letter, we report the products of reacting ions such as NO^+, NH_4^+, NO_3^-, and O_2^- with vaporized aprotic ionic liquids in their intact ion pair form. Ion pair fragmentation to the cation or anion as well as ion exchange and ion addition processes are observed by selected-ion flow tube mass spectrometry. Free energies of the reactions involving 1-ethyl-3-methylimidazolium bis-trifluoromethylsulfonylimide determined by ab initio quantum mechanical calculations indicate that ion exchange or ion addition are energetically more favorable than charge-transfer processes, whereas charge-transfer processes can be important in reactions involving 1-butyl-3-methylimidazolium dicyanamide.

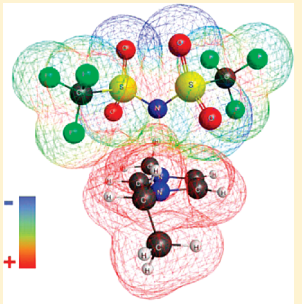

gas phase structure of an ion pair of $EMIM^+NTf_2^-$ ionic liquid

SECTION: Kinetics, Spectroscopy

Due to the high heats of vaporization involved with room-temperature ionic liquids (RTILs), direct detection of RTIL vapors has proved difficult. Primary attempts to detect ionic liquid vapors under reduced pressure and to understand the nature of their volatilization have focused on mass spectrometric methods[1−4] and, more recently, IR[5,6] and UV−vis spectroscopy.[7] Indirect methods involve transpiration,[8] effusion,[9] or thermal gravimetric analyses.[10,11] Protic ionic liquids (having a hydrogen on the ring nitrogen) tend to vaporize via proton transfer from the cation to the anion, and these molecular species have been shown to evaporate from the surface,[12−14] while aprotic ionic liquids (with alkylated ring nitrogens) have been shown to vaporize as intact ion pairs.[4,15,16] To our knowledge, only one prior study has directly detected evaporated intact ion pairs, albeit under rather harsh thermal conditions.[17] One drawback using positive mode ionization mass spectrometric techniques is that upon removing an electron from the ion pair, the Coulombic attraction between the cation and anion is lost, and the remaining attractive forces between the cation−radical complex can be weak, and the complex can easily dissociate to the cation and radical. It is the detection of the intact cation which implies the presence of ion pairs in the vapor phase.[4,15] If, instead of removing an electron from the anion in the ion pair, a third ion can be gently attached to the ion pair, this would enable the detection of the larger charged product via mass spectrometry. Previous work using electrospray ionization mass spectrometry (ESI-MS)[18] has detected multiple ion clusters, $(C^+)_nA^-_{(n-1)}$ in positive ion mode or $(C^+)_{(n-1)}A^-_{(n)}$ in negative ion mode. However, these clusters are formed under field evaporation conditions, not reduced pressure distillation conditions. Ion−ion pair reactions have been observed from reduced-pressure evaporation of ionic liquids by Fourier transform ion cyclotron resonance mass spectrometry (FT-ICR-MS).[16,19,20] In the FT-ICR-MS experiments, an evaporated ion pair dissociatively ionizes; the cation is trapped and can then add to another ion pair, forming stable clusters similar to those seen in ESI-MS experiments that are based on the original ionic liquid being evaporated.

The goal of this work was to expose vaporized ion pairs to different and more labile ions to look for intact RTIL ion pairs through proton transfer, charge exchange, clustering, or possible reactivity. Ions were chosen in order to observe (1) a protonated

Received: February 16, 2011
Accepted: March 24, 2011

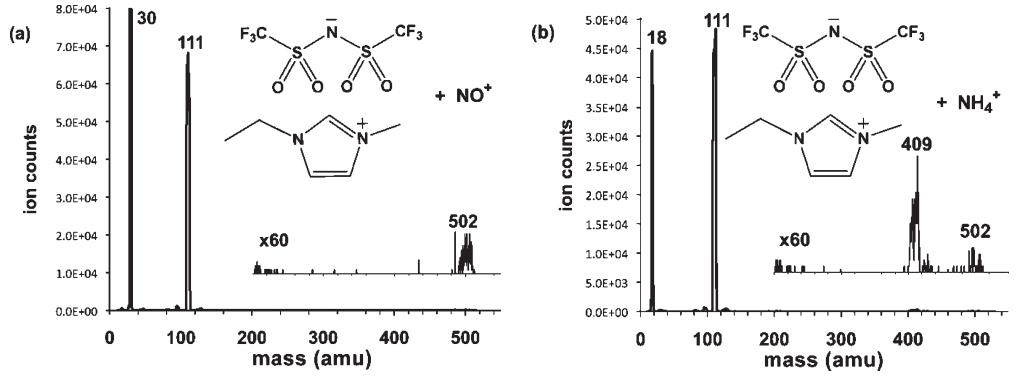

Figure 1. Positive ion mass spectra for the reactions (a) $EMIM^+NTf_2^-$ + NO^+ and (b) $EMIM^+NTf_2^-$ + NH_4^+.

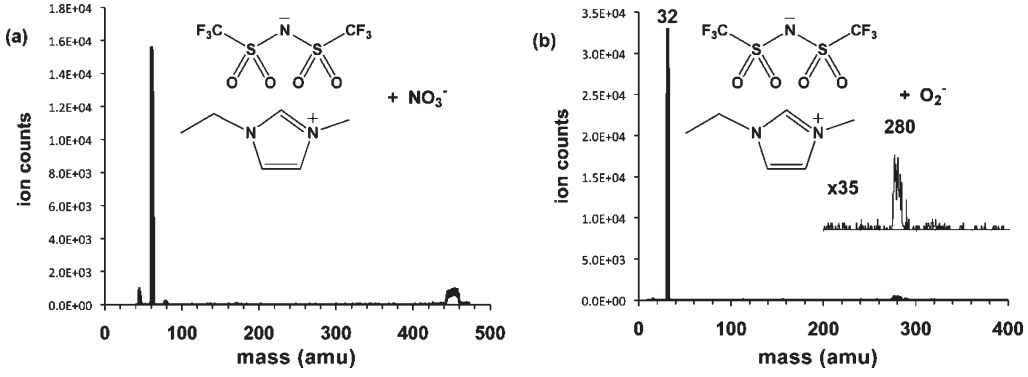

Figure 2. Negative ion mass spectra for the reactions (a) $EMIM^+NTf_2^-$ + NO_3^- and (b) $EMIM^+NTf_2^-$ + O_2^-.

ion pair via proton transfer from NH_4^+ (proton affinity (PA)(NH_3) = 8.85 eV[21]), (2) a negatively charged ion pair by electron transfer from O_2^- (electron affinity (EA)(O_2) = 0.45 eV[22]), and (3) soft chemical ionization of the ion pair by electron transfer from the ion pair to NO^+ (ionization potential (IP)(NO) = 9.27 eV[23]). The relative PAs, EAs, and IPs of the ion pairs should indicate potential reactivity with the above ions. Apparently, the Coulombic energy gained by ion addition or ion exchange with 1-ethyl-3-methylimidazolium bis-trifluoromethylsulfonylimide ($EMIM^+NTf_2^-$) can dominate the possible charge-transfer processes, whereas charge transfer is more likely occurring with 1-butyl-3-methylimidazolium dicyanamide ($BMIM^+dca^-$).

Experiments were performed in the AFRL-Hanscom selected-ion flow tube (SIFT) mass spectrometric apparatus, which has been modified to introduce an effusive RTIL source. In order to produce conditions that most likely would aid in the observation of intact ion pairs, the flow tube was cooled to 170 K. The reactions of NO^+, NH_4^+, NO_3^-, and O_2^- with the vaporized ionic liquid $EMIM^+NTf_2^-$ and NO^+ and NH_4^+ with the vaporized ionic liquid $BMIM^+dca^-$ were monitored in positive ion mode for NO^+ and NH_4^+ and in negative ion mode for NO_3^- (EA(NO_3) = 3.937 eV)[22] and O_2^- ions. When $EMIM^+NTf_2^-$ (mass 391, IP = 8.23 eV (MP2/6-311++G(d,p)) is reacted with NO^+ or NH_4^+, the major ion detected is mass 111, the $EMIM^+$ cation, seen in Figure 1a and b. A small product peak also appears at mass 502, corresponding to the secondary reaction $EMIM^+ + EMIM^+NTf_2^- \rightarrow EMIM^+NTf_2^-EMIM^+$. For NH_4^+, a mass peak at 409 corresponding to $EMIM^+$-$NTf_2^-NH_4^+$ is also detected (Figure 1b). $EMIM^+NTf_2^-$ + NO_3^- yields a mass at 453, corresponding to $NO_3^-EMIM^+$-NTf_2^- (Figure 2a). When $EMIM^+NTf_2^-$ is reacted with O_2^-, the major ion detected is mass 280, the NTf_2^- anion, seen in Figure 2b. Possible reactions involved in the formation of the ions that correspond to the experimental mass peaks observed for $EMIM^+NTf_2^-$ are listed in Table 1, along with their enthalpies and free energies of reaction (at 298 K).

In the cases when $EMIM^+NTf_2^-$ is reacted with NO^+ or NH_4^+, the $EMIM^+$ (mass 111) ion is readily formed, presumably through a $C_i^+A^-C_j^+$ type of intermediate which dissociates to the $EMIM^+$ cation plus a cofragment, either an ion pair, $NO^+NTf_2^-$, or a hydrogen-bonded complex, NH_3HNTf_2, which are predicted to be exergonic (ΔG = −35.9 and −25.6 kcal/mol, reactions 2 and 5, Table 1). Because masses 391 or 392 were not detected, simple charge transfer via electron removal or proton attachment to the ion pair apparently is not an important process. The relatively high concentration of $EMIM^+$ cation produced can then react in a secondary process with the RTIL ion pair to form an $EMIM^+NTf_2^-EMIM^+$ ion trio (ΔG = −21.2 kcal/mol, reaction 13, Table 1) at mass 502. Although reaction 13 is less exergonic than reaction 2 due to entropic contributions, that is, reaction 13 is the combination of two particles whereas reaction 2 conserves the number of particles involved in the reaction, the apparent preference for reaction 2 products over reaction 13 products is explained by sequential kinetics. Assuming negligible mass 502 loss rates, its yield is determined by the rate of production of mass 111 in reaction 2. The formation of the NTf_2^- anion is also observed upon reaction of $EMIM^+NTf_2^-$ with O_2^-, but the formation of $NTf_2^-EMIM^+NTf_2^-$ (mass

dx.doi.org/10.1021/jz200212j |J. Phys. Chem. Lett. 2011, 2, 874–879

Table 1. Enthalpies and Free Energies of Reaction of the RTILs $EMIM^+NTf_2^-$ and $BMIM^+dca^-$ with Various Ions at 298 K (MP2/6-311++G(d,p))

	reaction	ΔH (298 K) (kcal/mol)	ΔG (298 K) (kcal/mol)	mass (amu)[a]
(1)	$EMIM^+NTf_2^- + NO^+ \rightarrow EMIM^+ + NTf_2 + NO$	3.6	−11.0	111
(2)	$EMIM^+NTf_2^- + NO^+ \rightarrow EMIM^+ + NO^+NTf_2^-$	−32.8	−35.9	111
(3)	$EMIM^+NTf_2^- + NO^+ \rightarrow EMIM^+NTf_2^-NO^+$	−53.6(−53.9)[b]	−44.6(−48.5)[b]	421
(4)	$EMIM^+NTf_2^- + NH_4^+ \rightarrow EMIM^+ + HNTf_2 + NH_3$	−3.3(−3.1)[b]	−17.4(−11.3)[b]	111
(5)	$EMIM^+NTf_2^- + NH_4^+ \rightarrow EMIM^+ + NH_3HNTf_2$	−19.8	−25.6	111
(6)	$EMIM^+NTf_2^- + NH_4^+ \rightarrow EMIM^+ + NTf_2 + NH_4$	117.5	103.0	111
(7)	$EMIM^+NTf_2^- + NH_4^+ \rightarrow EMIM^+NTf_2^-NH_4^+$	−47.7	−40.8	409
(8)	$EMIM^+NTf_2^- + NO_3^- \rightarrow NO_3^-EMIM^+NTf_2^-$	−36.3	−28.0	453
(9)	$EMIM^+NTf_2^- + O_2^- \rightarrow NTf_2^- + EMIM{:}HO_2$	8.9(9.1)[b]	3.9(6.1)[b]	280
(10)	$EMIM^+NTf_2^- + O_2^- \rightarrow NTf_2^- + EMIM^+O_2^-$	13.4	10.3	280
(11)	$EMIM^+NTf_2^- + O_2^- \rightarrow NTf_2^- + EMIM{:} + HO_2$	27.1	13.0	280
(12)	$EMIM^+NTf_2^- + O_2^- \rightarrow NTf_2^- + EMIM + O_2$	24.7	12.1	280
(13)	$EMIM^+NTf_2^- + EMIM^+ \rightarrow EMIM^+NTf_2^-EMIM^+$	−32.4(−32.8)[b]	−21.2(−26.1)[b]	502
(14)	$BMIM^+dca^- + NO^+ \rightarrow BMIM^+ + dca + NO$	−35.0	−47.6	139
(15)	$BMIM^+dca^- + NO^+ \rightarrow BMIM^+ + NO^+dca^-$	−40.9	−43.2	139
(16)	$BMIM^+dca^- + NO^+ \rightarrow BMIM^+NO + dca$	−22.6	−28.3	169
(17)	$BMIM^+dca^- + NH_4^+ \rightarrow BMIM^+ + dca + NH_4$	79.0	66.4	139
(18)	$BMIM^+dca^- + NH_4^+ \rightarrow BMIM^+ + NH_4^+dca^-$	−27.9	−32.1	139

[a] The mass (amu) column indicates the mass of the detected ion, except for reaction 3, which is not observed experimentally. The EMIM carbene species in reaction 11 is denoted as EMIM. [b] Values in parentheses are calculated at T = 170 K.

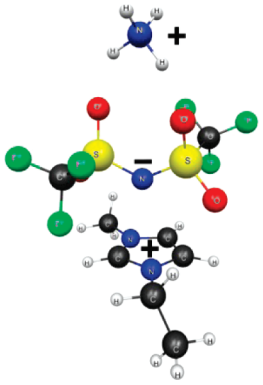

Figure 3. $NH_4^+NTf_2^-EMIM^+$ ion cluster geometry.

671) or larger cluster ions cannot be detected as they are out of the mass range of the present detector (amu ≤ 600). The coproduct of the NTf_2^- anion formed upon reaction with O_2^- is unclear. Some of the possible processes considered (reactions 9−12, Table 1) all appear to be endergonic, although the formation of the HO_2/EMIM carbene[24] complex product (reaction 9) has a ΔG of only +3.9 ± 10 kcal/mol and therefore would be the most likely route among reactions 9−12. The lack of signal at mass 391 suggests that electron transfer from O_2^- or NO_3^- is not an important process. Finally, small ion signals corresponding to ion addition to the ion pair are observed when $EMIM^+NTf_2^-$ is reacted with NH_4^+ or NO_3^-, resulting in $EMIM^+NTf_2^-NH_4^+$ (mass 409, ΔG = −40.8 kcal/mol) or $NO_3^-EMIM^+NTf_2^-$ (mass 453, ΔG = −28.0 kcal/mol) in reactions 7 and 8, respectively. Detection of the ion trio definitely shows the presence of neutral RTIL vapors in the flow tube. The calculated geometry of $EMIM^+NTf_2^-NH_4^+$ in Figure 3 shows a dramatic change in geometry of the $EMIM^+NTf_2^-$ from the previously calculated geometries[5,25] upon addition of NH_4^+. The NTf_2^- migrates from being essentially coplanar with the $EMIM^+$ ring in the ion pair to being perpendicular to the ring and is sandwiched between the $EMIM^+$ and NH_4^+ cations in the $EMIM^+NTf_2^-NH_4^+$ ion trio. Some excess internal energy gained upon ion addition to the ion pair can be removed by collisions with the buffer gas at 170 K, which is consistent with the absence of the complex under room-temperature conditions, indicating that the bonds holding the complex together are weak. However, more exergonic processes may not be observed at 170 K if the dissociation rate of the internally excited complex is faster than thermalization by collisional de-excitation, which could be the case for $EMIM^+NTf_2^-NO^+$ (mass 421, ΔG = −44.6 kcal/mol, reaction 3) and may explain why the $EMIM^+NTf_2^-NH_4^+$ signal (reaction 7) is less than the $EMIM^+$ signal (reactions 4−5) even though reaction 7 is more exergonic. Although the reaction enthalpies and free energies in Table 1 are reported under standard conditions at 298 K, several calculations were also performed at 170 K as in reactions 3, 4, 9, and 13 in order to determine how much the 298 K values deviate from the experimental conditions. These reactions were selected to account for the differences in entropic contributions going from two reactant particles to one product (reactions 3 and 13), to two products (reaction 9), or to three products (reaction 4). The observed changes in ΔG by −3.9, +2.2, and +6.1 kcal/mol, respectively, are all within the estimated uncertainty of ±10 kcal/mol.

When $BMIM^+dca^-$ (IP = 7.4 eV, MP2/6-311++G(d,p)//B3LYP/6-311++G(d,p)) is reacted with NH_4^+, mass peaks include 139, 96, 125, and 82 (Figure 4a). For the corresponding reaction with NO^+, mass peaks appear at 139, 125, 169, 179, 155, and 152 (Figure 4b). The observation of a peak at mass 139 indicates the formation of the $BMIM^+$ cation in these two reactions. Similar to the $EMIM^+NTf_2^-$ system, this could be from the dissociation of the $C_i^+A^-C_j^+$ intermediate ($BMIM^+dca^-NO^+$ or $BMIM^+dca^-NH_4^+$). However, unlike the $EMIM^+NTf_2^-$ system, no peaks were detected corresponding

dx.doi.org/10.1021/jz200212j |J. Phys. Chem. Lett. 2011, 2, 874–879

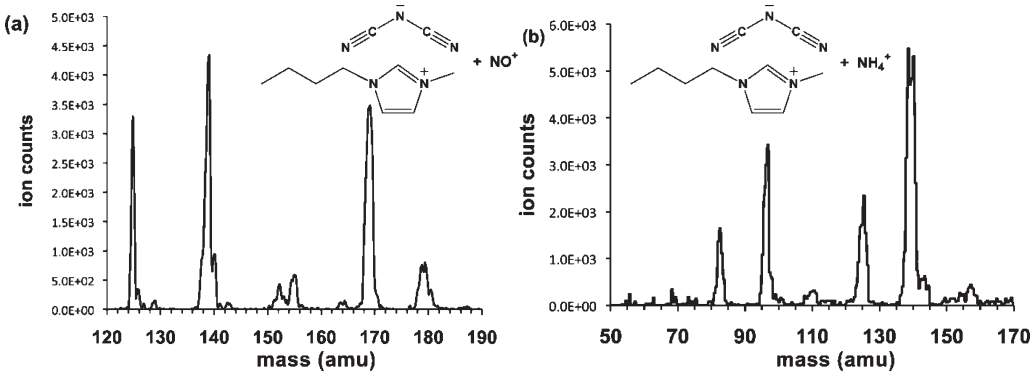

Figure 4. Positive ion mass spectra for the reactions of (a) $BMIM^+dca^-$ + NO^+ and (b) $BMIM^+dca^-$ + NH_4^+.

to the secondary product $BMIM^+dca^-BMIM^+$ at mass 344. This could be due to the lower vapor pressure, and thus lower concentration, of $BMIM^+dca^-$ in the flow tube or weaker bonds. The presence of peaks with masses less than 139 could be due to fragmentation of the $BMIM^+$ cation as masses 82, 96, and 125 are seen in photoionization studies of $BMIM^+dca^-$.[26] The complexity of the $BMIM^+dca^-$ mass spectra is likely due to the increased free-energy release from charge-transfer reactions compared to the similar charge-transfer reactions in the $EMIM^+NTf_2^-$ system (reactions 1 and 5, Table 1). In fact, electron transfer (reaction 14) is favored over ion exchange (reaction 15) by 4.4 kcal/mol. The large free energy released from electron transfer likely leads to fragmentation of the $BMIM^+$ cation, though reactions with impurities are not ruled out. The remaining mass peaks above mass 139 may result from more complex chemistry involving ion-neutral interactions such as in reaction 16 or reactions with impurities, and this will be addressed in a future publication.

This work reports the experimental results of reacting vaporized ionic liquids $EMIM^+NTf_2^-$ and $BMIM^+dca^-$ with various ions including NO^+, NH_4^+, NO_3^-, and O_2^-. The presence of intact $EMIM^+NTf_2^-$ ion pairs in the gas phase is evidenced by the ion cluster (mass 502) formation seen in Figures 1 and 2. The presence of intact $BMIM^+dca^-$ ion pairs in the gas phase is less direct and indicated by the formation of the intact $BMIM^+$ cation (mass 139) seen in Figure 4. This experimental technique enables the examination of the influence of various energetic factors such as proton affinity, electron affinity, and ionization potential of the reactants on the outcome of the reactivity of vaporized RTIL ion pairs with reagent ions. While dissociation to the cation or anion, ion exchange, or ion addition dominate for the $EMIM^+NTf_2^-$—ion reactions, more complex reactivity is observed for the $BMIM^+dca^-$—ion reactions. More experimental and theoretical work is needed to evaluate these influences in RTIL ion pair—ion reactions.

EXPERIMENTAL SECTION

The measurements were carried out using the Air Force Research Laboratory selected ion flow tube (SIFT), which has been well described in detail previously.[27] Ions are made in a high-pressure ion source by electron impact, mass selected in a quadrupole mass filter, and injected into a helium-buffered flow tube through a Venturi inlet. Source gases were O_2 for O_2^-, HNO_3 for NO_3^-, NO or NO_2 for NO^+, and NH_3 for NH_4^+. In all cases, the primary ion accounted for >95% of all signal in the absence of the added ionic liquid. The helium carries the primary ions past a neutral inlet, and the core of the flow is sampled into a quadrupole mass spectrometer for ion identification. The pressure inside of the flow tube is 0.5 Torr. Because one of the main aims of the present experiments was to observe intact ion pairs whose ionized forms can readily dissociate, we ran the flow tube at 170 K to minimize thermal dissociation of the ions. The mass spectrometer was calibrated with C_7F_4, and the masses are accurate to 1 amu. Peak broadening at higher masses is due to the limited resolution of the mass spectrometer under experimental conditions, and high masses are confirmed to be single peaks and not distributions of peaks. The differences in the relative loss rates of ions from diffusion and wall reactions are expected to be small, and because we are not reporting rate constants or absolute yields, these corrections were not considered in the reported figures.

What is described above is quite standard and straightforward for the SIFT. What is more challenging is to introduce ionic liquids into the flow tube because their vapor pressure is low.[9,28] The inlet is similar to one that we have used for sulfuric acid.[29] A 1/4 in. glass tube is wrapped with insulated heating wire in two zones, a short one near the tip and a longer one covering most of the inlet. Resistance temperature detectors measure the temperature of the glass tube in each zone. The inlet extends into the center of the flow tube. Because the SIFT has a unipolar plasma that charges insulating surfaces, the whole inlet is wrapped by a stainless steel shim connected to ground. Glass wool is inserted inside of the length of the glass tube, and a small amount of ionic liquid is distributed throughout the glass wool by syringe injection. Helium flush gas of up to 145 sccm was used to transport the ionic liquid to the flow tube, and a He flow of 10 000 sccm was present in the SIFT.

Before introducing a new RTIL sample into the SIFT apparatus, methanol was used to thoroughly clean the inlet; the inlet was dried, and new glass wool was inserted. The temperature of the inlet was kept at approximately 433 and 453 K for $BMIM^+dca^-$ and $EMIM^+NTf_2^-$, respectively. Preliminary measurements indicated that it was easy to overheat and pyrolyze the RTIL; therefore, heating was done slowly.

Two types of data were taken, (1) mass spectra with a constant helium flow, and (2) peak stepping through all relevant peaks (minor peaks of ~1−2% were excluded) as a function of the helium flow. The latter data were taken to look for secondary reactions. As the flow of helium increased, the flow of ionic liquid also increased. In order to account for potential secondary reactions such as reaction 13, we used the standard SIFT method[30] of plotting the fraction of each product versus the

dx.doi.org/10.1021/jz200212j |J. Phys. Chem. Lett. 2011, 2, 874–879

neutral flow rate (in this case, the He flush gas plots are standard and not shown). Extrapolations of the branching to zero flow yield primary branching fractions; negative slopes indicate product ions that further react with the RTIL, and positive slopes indicate products formed by secondary chemistry.

Although the vapor pressures of the ILs can be estimated[28] and are thought to be in the range of 0.01−0.1 mTorr, we did not attempt to measure rate constants. However, for all species, the product abundances appeared roughly constant for the same He flow through the inlet, indicating that the rates were similar and fast, that is, near the collision rate.

The ab initio calculations were performed at the MP2/6-311++G(d,p) and B3LYP/6-311++G(d,p) levels of theory[31−40] using the GAMESS[41,42] quantum chemistry code. Reaction enthalpies and free energies (MP2) were computed using the ideal gas + rigid rotor + harmonic oscillator models[37] with the computed vibrational frequencies scaled by a factor of 0.9748.[40] For the dca neutral doublet (reactions 14, 16, and 17), due to convergence problems at the MP2 level, the MP2/6-311++G-(d,p) energy was obtained as a single-point calculation at the B3LYP/6-311++G(d,p) optimized geometry, and B3LYP scaled harmonic frequencies (scale factor = 0.9806) were used for the ZPE and thermal/entropic corrections. The uncertainty assigned to the calculated reaction enthalpies in Table 1 is ±10 kcal/mol, which was obtained by the procedure described in the Supporting Information.

■ ASSOCIATED CONTENT

Supporting Information. In order to estimate the uncertainty in the MP2 calculations in Table 1, reaction energies using MP2/aug-cc-pvtz and CCSD(T)/6-311++G(d,p) single-point energies were computed. This material is available free of charge via the Internet at http://pubs.acs.org.

■ AUTHOR INFORMATION

Corresponding Author

*E-mail: ghanshyam.vaghjiani@edwards.af.mil. Tel: 661-275-5657. Fax: 661-275-5471.

■ ACKNOWLEDGMENT

Funding for this work was provided by the Air Force Office of Scientific Research under Contract No. FA9300-06-C-0023 for the Air Force Research Laboratory, Edwards AFB, CA 93524. A. A.V. is grateful for support from AFOSR under Project 2303EP4. J.F.F. and N.E. acknowledge funding from the Institute for Scientific Research of Boston College (FA8718-04-C-0055). This work was supported in part by a grant of computer time from the Department of Defense (DoD) High Performance Computing Modernization Program at the Army Research Laboratory, the Air Force Research Laboratory, Engineer Research and Development Center, and Navy DoD Supercomputing Resource Centers (DSRCs).

■ REFERENCES

(1) Emel'yanenko, V. N.; Verevkin, S. P.; Heintz, A.; Corfield, J.-A.; Deyko, A.; Lovelock, K. R. J.; Licence, P.; Jones, R. G. Pyrrolidinium-Based Ionic Liquids. 1-Butyl-2-methyl Pyrroldinium Dicyanoamide: Thermochemical Measurement, Mass Spectrometry, and Ab Initio Calculations. *J. Phys. Chem. B* **2008**, *112*, 11734–11742.

(2) Lovelock, K. R. J.; Deyko, A.; Licence, P.; Jones, R. G. Vaporisation of an Ionic Liquid Near Room Temperature. *Phys. Chem. Chem. Phys.* **2010**, *12*, 8893–8901.

(3) Strasser, D.; Goulay, F.; Belau, L.; Kostko, O.; Koh, C.; Chambreau, S. D.; Vaghjiani, G. L.; Ahmed, M.; Leone, S. R. Tunable Wavelength Soft Photoionization of Ionic Liquid Vapors. *J. Phys. Chem. A* **2010**, *114*, 879–883.

(4) Strasser, D.; Goulay, F.; Kelkar, M. S.; Maginn, E. J.; Leone, S. R. Photoelectron Spectrum of Isolated Ion-Pairs in Ionic Liquid Vapor. *J. Phys. Chem. A* **2007**, *111*, 3191–3915.

(5) Akai, N.; Parazs, D.; Kawai, A.; Shibuya, K. Cryogenic Neon Matrix-Isolation FTIR Spectroscopy of Evaporated Ionic Liquids: Geometrical Structure of Cation−Anion 1:1 Pair in the Gas Phase. *J. Phys. Chem. B* **2009**, *113*, 4756–4762.

(6) Fumino, K.; Wulf, A.; Verevkin, S. P.; Heintz, A.; Ludwig, R. Estimating Enthalpies of Vaporization of Imidazolium-Based Ionic Liquids from Far-Infrared Measurements. *ChemPhysChem* **2010**, *11*, 1623–1626.

(7) Wang, C.; Luo, H.; Li, H.; Dai, S. Direct UV-Spectroscopic Measurement of Selected Ionic-Liquid Vapors. *Phys. Chem. Chem. Phys.* **2010**, *12*, 7246–7250.

(8) Verevkin, S. P.; Emel'yanenko, V. N.; Zaitsau, D. H.; Heintz, A.; Muzny, C. D.; Frenkel, M. Thermochemistry of Imidazolium-Based Ionic Liquids: Experiment and First-Principles Calculations. *Phys. Chem. Chem. Phys.* **2010**, *12*, 14994–15000.

(9) Zaitsau, D. H.; Kabo, G. J.; Strechan, A. A.; Paulechka, Y. U.; Tscherisch, A.; Verevkin, S. P.; Heintz, A. Experimental Vapor Pressures of 1-Alkyl-3-methylimidazolium Bis(trifluoromethylsulfonyl)imides and a Correlation Scheme for Estimation of Vaporization Enthalpies of Ionic Liquids. *J. Phys. Chem. A* **2006**, *110*, 7303–7306.

(10) Wooster, T. J.; Johanson, K. M.; Fraser, K. J.; MacFarlane, D. R.; Scott, J. L. Thermal Degradation of Cyano Containing Ionic Liquids. *Green Chem.* **2006**, *8*, 691–696.

(11) Ngo, H. L.; LeCompte, K.; Hargens, L.; McEwen, A. B. Thermal Properties of Imidazolium Ionic Liquids. *Thermochim. Acta* **2000**, *357−358*, 97–102.

(12) Earle, M. J.; Esperança, J. M. S. S.; Gilea, M. A.; Canongia Lopes, J. N.; Rebelo, L. P. N.; Magee, J. W.; Seddon, K. R.; Widegren, J. A. The Distillation and Volatility of Ionic Liquids. *Nature* **2006**, *439*, 831–834.

(13) Kreher, U. P.; Rosamilia, A. E.; Raston, C. L.; Scott, J. L.; Strauss, C. R. Self-Associated "Distillable" Ionic Media. *Molecules* **2004**, *9*, 387–393.

(14) Yoshizawa, M.; Xu, W.; Angell, C. A. Ionic Liquids by Proton Transfer: Vapor Pressure, Conductivity, and the Relevance of pKa from Aqueous Solutions. *J. Am. Chem. Soc.* **2003**, *125*, 15411–15419.

(15) Armstrong, J. P.; Hurst, C.; Jones, R. G.; Licence, P.; Lovelock, K. R. J.; Satterly, C. J.; Villar-Garcia, I. J. Vapourisation of Ionic Liquids. *Phys. Chem. Chem. Phys.* **2007**, *9*, 982–990.

(16) Leal, J. P.; Esperança, J. M. S. S.; Minas da Piedade, M. E.; Canongia Lopes, J. N.; Rebelo, L. P. N.; Seddon, K. R. The Nature of Ionic Liquids in the Gas Phase. *J. Phys. Chem. A* **2007**, *111*, 6176–6182.

(17) Gross, J. H. Molecular Ions of Ionic Liquids in the Gas Phase. *J. Am. Soc. Mass Spectrom.* **2008**, *19*, 1347–1352.

(18) Chiu, Y.-H.; Gaeta, G.; Heine, T. R.; Dressler, R. A.; Levandier, D. J. Analysis of the Electrospray Plume from the EMI-Im Propellant Externally Wetted on a Tungsten Needle. In *42nd AIAA/ASME/SAE/ASEE Joint Propulsion Conference*; Sacramento, CA, 2006.

(19) Berg, R. W.; Riisager, A.; Fehrmann, R. Formation of an Ion-Pair Molecule with a Single $NH^{+}\cdots Cl^{-}$ Hydrogen Bond: Raman Spectra of 1,1,3,3-Tetramethylguanidinium Chloride in the Solid State, in Solution, and in the Vapor Phase. *J. Phys. Chem. A* **2008**, *112*, 8585–8592.

(20) Vitorino, J.; Leal, J. P.; Minas da Piedade, M. E.; Canongia Lopes, J. N.; Esperança, J. M. S. S.; Rebelo, L. s. P. N. The Nature of Protic Ionic Liquids in the Gas Phase Revisited: Fourier Transform Ion Cyclotron Resonance Mass Spectrometry Study of 1,1,3,3-Tetramethylguanidinium Chloride. *J. Phys. Chem. B* **2010**, *114*, 8905–8909.

(21) Hunter, E. P.; Lias, S. G. Proton Affinity Evaluation. In *NIST Chemistry WebBook*, NIST Standard Reference Database Number 69; Linstrom, P. J., Mallard, W. G., Eds.; National Institute of Standards and Technology: Gaithersburg, MD, http://webbook.nist.gov/chemistry/ (accessed February 2011).

(22) Bartmess, J. E. Negative Ion Energetics Data. In *NIST Chemistry WebBook*, NIST Standard Reference Database Number 69; Linstrom, P. J., Mallard, W. G., Eds.; National Institute of Standards and Technology: Gaithersburg, MD, http://webbook.nist.gov/chemistry/ (accessed February 2011).

(23) Lias, S. G. Ionization Energy Evaluation. In *NIST Chemistry WebBook*, NIST Standard Reference Database Number 69; Linstrom, P. J., Mallard, W. G., Eds.; National Institute of Standards and Technology: Gaithersburg, MD, http://webbook.nist.gov/chemistry/ (accessed February 2011).

(24) Holloczki, O.; Gerhard, D.; Massone, K.; Szarvas, L.; Nemeth, B.; Veszpremi, T.; Nyulaszi, L. Carbenes in Ionic Liquids. *New J. Chem.* **2010**, *34*, 3004–3009.

(25) Paulechka, Y. U.; Kabo, A. G.; Emel'yanenko, V. N. Structure, Conformations, Vibrations, and Ideal-Gas Properties of 1-Alkyl-3-methylimidazolium Bis(trifluoromethylsulfonyl)imide Ionic Pairs and Constituent Ions. *J. Phys. Chem. B* **2008**, *112*, 15708–15717.

(26) Chambreau, S. D.; Vaghjiani, G. L.; To, A.; Koh, C.; Strasser, D.; Kostko, O.; Leone, S. R. Heats of Vaporization of Room Temperature Ionic Liquids by Tunable Vacuum Ultraviolet Photoionization. *J. Phys. Chem. B* **2010**, *114*, 1361–1367.

(27) Viggiano, A. A.; Morris, R. A.; Dale, F.; Paulson, J. F.; Giles, K.; Smith, D.; Su, T. Kinetic Energy, Temperature, Rotational Temperature Dependences for the Reactions of $Kr^+(^2P_{3/2})$ and Ar^+ with HCl. *J. Chem. Phys.* **1990**, *93*, 1149.

(28) Emel'yanenko, V. N.; Verevkin, S. P.; Heintz, A. The Gaseous Enthalpy of Formation of the Ionic Liquid 1-Butyl-3-methylimidazolium Dicyanamide from Combustion Calorimetry, Vapor Pressure Measurements, and Ab Initio Calculations. *J. Am. Chem. Soc.* **2007**, *129*, 3930–3937.

(29) Viggiano, A. A.; Seeley, J. V.; Mundis, P. L.; Williamson, J. S.; Morris, R. A. Rate Constants for the Reactions of $XO_3^-(H_2O)_n$ (X = C, HC, and N) and $NO_3^-(HNO_3)_n$ with H_2SO_4: Implications for Atmospheric Detection of H_2SO_4. *J. Phys. Chem. A* **1997**, *101*, 8275.

(30) Su, T.; Su, A. C. L.; Viggiano, A. A.; Paulson, J. F. Gas-Phase Ion−Molecule Reactions of Perfluoroolefins. *J. Phys. Chem.* **1987**, *91*, 3683–3685.

(31) Aikens, C. M.; Webb, S. P.; Bell, R.; Fletcher, G. D.; Schmidt, M. W.; Gordon, M. S. A Derivation of the Frozen-Orbital Unrestricted Open-Shell and Restricted Closed-Shell Second-Order Perturbation Theory Analytic Gradient Expressions. *Theor. Chim. Acta.* **2003**, *110*, 233–253.

(32) Bartlett, R. J.; Silver, D. M. Some Aspects of Diagrammatic Perturbation Theory. *Int. J. Quantum Chem.* **1975**, *S9*, 183–198.

(33) Clark, T.; Chandrasekhar, J.; Spitznagel, G. W.; Schleyer, P. v. R. Efficient Diffuse Function-Augmented Basis Sets for Anion Calculations. III. The 3-21+G Basis Set for First-Row Elements, Li−F. *J. Comput. Chem.* **1983**, *4*, 294–301.

(34) Frisch, M. J. e. a.; Head-Gordon, M. J.; Pople, J. A. A Direct MP2 Gradient Method. *Chem. Phys. Lett.* **1990**, *166*, 275–280.

(35) Hariharan, P. C.; Pople, J. A. The Influence of Polarization Functions on Molecular Orbital Hydrogenation Energies. *Theor. Chim. Acta.* **1973**, *28*, 213–222.

(36) Krishnan, R.; Binkley, J. S.; Seeger, R.; Pople, J. A. Self-Consistent Molecular Orbital Methods. XX. A Basis Set for Correlated Wave Functions. *J. Chem. Phys.* **1980**, *72*, 650–654.

(37) *Statistical Mechanics*; McQuarrie, D. A.; Woods, J. A., Eds.; Harper & Row: New York, 1976.

(38) Moller, C.; Plesset, M. S. Note on an Approximation Treatment for Many-Electron Systems. *Phys. Rev.* **1934**, *46*, 618–622.

(39) Pople, J. A.; Binkley, J. S.; Seeger, R. Theoretical Models Incorporating Electron Correlation. *Int. J. Quantum Chem.* **1976**, *S10*, 1–19.

(40) Scott, A. P.; Radom, L. Harmonic Vibrational Frequencies: An Evaluation of Hartree−Fock, Møller−Plesset, Quadratic Configuration Interaction, Density Functional Theory, and Semiempirical Scale Factors. *J. Phys. Chem.* **1996**, *100*, 16502–16513.

(41) Schmidt, M. W.; Baldridge, K. K.; Boatz, J. A.; Elbert, S. T.; Gordon, M. S.; Jensen, J. H.; Koseki, S.; Matsunaga, N.; Nguyen, K. A.; Su, S.; et al. General Atomic and Molecular Electronic Structure System. *J. Comput. Chem.* **1993**, *14*, 1347–1363.

(42) Gordon, M. S.; Schmidt, M. W. Advances in Electronic Structure Theory: GAMESS a Decade Later. In *Theory and Applications of Computational Chemistry: The First Forty Years*; Dykstra, C. E., Frenking, G., Kim, K. S., Scuseria, G. E., Eds.; Elsevier: Amsterdam, The Netherlands, 2005; pp 1167−1189.